



## TRUEFOOD

### Traditional United Europe Food

Contract no. FOOD-CT-2006-016264

Instrument: Integrated Project

Thematic Priority: Food Quality and Safety (# 5)

**D6.2.1.2 Robustness analysis of the models developed for the concerned applications (cheese mass loss observed during ripening) and generalisation.**

Due date of deliverable: March 2010  
Actual submission date : March 2010

Start date of project: 1 May 2006

Duration: 48 months

Organisation name of lead contractor for this deliverable : ACTIA

Revision : 1

Project co-funded by the European Commission within the Sixth Framework Programme (2002-2006)		
Dissemination Level		
PU	Public	
PP	Restricted to other programme participants (including the Commission Services)	X
RE	Restricted to a group specified by the consortium (including the Commission Services)	
CO	Confidential, only for members of the consortium (including the Commission Services)	

# **Robustness analysis of the models developed for the concerned applications (cheese mass loss observed during ripening) and generalisation.**

Epistemic and stochastic uncertainty processing in the modelling of cheese mass loss during ripening.

S. Gaucel, C. Baudrit, H. Guillemin, G. Corrieu.

INRA - UMR GMPA  
F - 78850 Thiverval Grignon

## **Summary**

In a knowledge integration approach, the work performed is focused on modelling, representation and propagation of uncertainties - on expert knowledge and sensors measurements - for a food transformation process. The aim was to analyse the robustness of a generalised model designed to study the cheese mass loss during the ripening process in a closed atmosphere. This generalised model was built to estimate the mass loss of a Camembert as a soft cheese and Saint Nectaire as a semi hard cheese.

According to the knowledge of experts about the cheese ripening, relative humidity of the ripening chamber, heat and mass transfer coefficients and cheese surface water activity were identified as the model input variables and parameters subject to the strongest imprecision and/or variability. A propagation of these uncertainties along the cheese mass loss model was performed - for 8 Camembert trials and 2 Saint Nectaire trials - to improve the generalization character of such a model. It provided the minimal and maximal cheese mass losses, according to the ripening conditions and the included knowledge. For Camembert type cheese, the length of the cheese mass loss ranges vary from 14.2 g - for low water exchange and biological activity - to 71.6 g - for high water exchange and biological activity. Results for the Saint Nectaire experiments leads to length of the mass loss ranges close to 300g.

Finally, these results confirm the legitimacy and merits of this approach in order to perform generalisation for cheese ripening process and potentially for a larger range of food transformation processes.

## **1 Introduction**

The ripening process is one most important steps for many cheese makers. Microbial activities and physico-chemical changes responsible for the organoleptic characteristics of cheeses are influenced by the climatic conditions of ripening chambers (temperature, relative humidity and the gas

composition of the air). Cheese mass loss dynamic is an integrative variable that introduces the production evolution. It is a key point in the ripening process, with consequences on productivity and a risk that the resulting product may be dropped in status (for example, the Camembert-Normandie protected designation of origin requires a final weight of 0.25 kg with between 105 and 115 mm diameter by 30 mm thick). Ventilation is used to evacuate heat and humidity generated by cheeses and the spatial distribution of climatic conditions inside cheese-ripening rooms is dependent on airflow (air velocity, air change rate).

In a first step of the work, focused on expertise elicitation, a qualitative survey was designed and the work methods used by expert operators in charge of the cheese ripening processes were identified. The information collected was then represented on a correspondence analysis map. Results showed that controlling cheese ripening processes requires careful monitoring during certain stages (see Deliverable D6.2.1.1 "A cognitive map about the knowledge of the experts for the concerned applications and a general methodology to deal with expertise"). The method built could be implemented in the cheese industry in order to train new operators. It may also open the way for research projects aimed at creating a model of the cheese ripening process.

A model was built to estimate the mass loss of a Camembert as a soft cheese and Saint Nectaire a semi hard cheese during the ripening process in a closed atmosphere (see Deliverable D2A.3.8 - Mathematical model describing the dynamic of the Saint-Nectaire cheese type weight loss as a function of key environmental variables acting on the process. Proposition of ripening conditions improving the process).

The model is based on the combination of three phenomena: water evaporation; convective and radiant exchanges and respiratory activity. It is composed of two equations with four input variables (relative humidity  $rh$ , atmospheric temperature  $T_\infty$ , oxygen consumption rate  $r_{O_2}$ , and carbon dioxide production rate  $r_{CO_2}$ ); two state variables (cheese mass  $m$ , surface temperature  $T_s$ ) and several parameters listed in Table 2.

Heat and mass transfers have been extensively studied in relation to cooking and drying processes. However, little data have been published in the case of cheese ripening, and transfer coefficients between the cheese and the atmosphere are not precisely described. Heat and mass transfer coefficients depend on cheese shapes and airflow velocities. Associated with the ill-known airflow distribution inside ripening chambers, we are thus faced with imprecise and incomplete knowledge relative to the spatial variability of climatic conditions, heat and water transfer coefficients. These considerations, plus the random nature of knowledge, lead to uncertainty that must be taken into account in the decision-making process. It is increasingly acknowledged that uncertainty regarding model parameters essentially has two origins (Ferson and Ginzburg, 1996). It may arise from randomness (often referred to as "stochastic uncertainty") due to the natural variability of observations resulting from heterogeneity or the fluctuations of a quantity over time. Or it may be caused by imprecision (often referred to as "epistemic uncertainty") due to a lack of information. This lack of knowledge may stem from a partial lack of data; either this data is impossible to collect, or only experts can provide some imprecise information. For example, it is quite common for experts to estimate the numerical values of parameters in the form of confidence intervals according to their experience and intuition. The uncertainty pervading model parameters is not just due to randomness; incomplete knowledge may coexist, especially as the result of the presence of several heterogeneous sources of knowledge such as statistical data and expert opinions, for example. The most commonly used theory for distinguishing incompleteness from randomness is that of imprecise probabilities developed at length by Walley (1991). In this theory, sets of probability distributions capture the notion of partial lack of probabilistic information.

While information regarding variability is best conveyed using probability distributions, information regarding imprecision is more accurately conveyed using families of probability distributions. Possibility distributions (also known as fuzzy intervals) (Dubois *et al.*, 2000) or belief functions introduced by Dempster (1967), and further elaborated by Shafer (1976) and Smets and Kennes (1994) in a different context, make it possible to encode such families.

Based on available knowledge about cheese ripening, the purpose was (i) to represent the information of model input variables and parameters subject to imprecision and/or variability; (ii) to jointly propagate randomness and imprecision through the model in order to estimate the uncertainty on model results (Baudrit *et al.*, 2007; Baudrit and Dubois, 2006). The aim was to demonstrate how a joint treatment of uncertainties can be useful for controlling the process even with few available instruments and to improve the generalization character of such models. This approach allows to evaluate the capacities of generalization of such models as regards to the resident uncertainty concerning (1) the knowledge on the ripening process that leads generally to biased parameters estimation, (2) imprecision on the sensor measurements, inputs of the model.

## 2 Nomenclature

$a_w$	Surface water activity (unitless)
$Bel$	Belief function
$C$	Specific heat ( $\text{J.kg}^{-1}.\text{K}^{-1}$ )
$h$	Heat transfer coefficient ( $\text{W.m}^{-2}.\text{K}^{-1}$ )
$k$	Mass (water) transfer coefficient ( $\text{kg.m}^{-2}.\text{Pa}^{-1}.\text{s}^{-1}$ )
$m$	Cheese mass(kg)
$N$	Necessity measure
$P$	Probability measure
$Pl$	Plausibility function
$P_{sv}(\cdot)$	Saturation vapour pressure (Pa)
$r_{CO_2}$	CO <sub>2</sub> product rates ( $\text{mol.m}^{-2}.\text{s}^{-1}$ )
$rh$	Relative humidity (unitless)
$r_{O_2}$	Oxygen consumption ( $\text{mol.m}^{-2}.\text{s}^{-1}$ )
$s$	Surface area of cheese ( $\text{m}^{-2}$ ) <sup>3</sup>
$T_s$	Surface temperature (K)
$T_\infty$	Atmospheric temperature (K)
$w_{CO_2}$	CO <sub>2</sub> molar mass ( $\text{kg.mol}^{-1}$ )
$w_{O_2}$	O <sub>2</sub> molar mass ( $\text{kg.mol}^{-1}$ )
$\alpha$	Respiration heat ( $\text{J.mol}^{-1}$ )
$\lambda$	Latent heat of water evaporation ( $\text{J.kg}^{-1}$ ) <sup>2</sup>
$\epsilon$	Product emissivity (unitless)
$\sigma$	Stefan-Boltzmann constant ( $\text{J.m}^{-2}.\text{K}^{-4}$ )
$\phi_r$	Respiration matter flux ( $\text{kg.m}^{-2}.\text{s}^{-1}$ )
$\phi_w$	Evaporative flux ( $\text{kg.m}^{-2}.\text{s}^{-1}$ )
$\psi_w$	Heat consumption flux ( $\text{J.m}^{-2}.\text{s}^{-1}$ )
$\psi_{cr}$	Heat exchange flux ( $\text{J.m}^{-2}.\text{s}^{-1}$ )
$\pi$	Possibility distribution
$\Pi$	Possibility measure
$\nu$	Mass distribution function

### 3 Uncertainty processing

#### 3.1 Basic notions of numerical possibility theory

Possibility theory (Dubois *et al.*, 2000) is useful for representing imprecise knowledge. A possibility distribution can model imprecise information regarding a fixed unknown parameter and it can also serve as an approximate representation of the incomplete observation of a random variable. The basic notion is the possibility distribution, referred to as  $\pi$ , describing the more or less plausible values of some uncertain variable. Let us consider an expert giving his opinion, for instance, on a heat transfer coefficient  $h$ . The expert is certain that  $h$  is located within the interval  $[2.86, 3.33]$   $\text{W.m}^{-2}.\text{K}^{-1}$  (see Figure 1). On the base of a few measurements and his own experience, the expert will be able to express preferences inside this interval (for example, the value of  $h$  is most likely between 3 and 3.2  $\text{W.m}^{-2}.\text{K}^{-1}$ ). Then, a possibility distribution  $\pi$  was defined (see Figure 1) telling that the most likely values (risky but informative values) for  $h$  are located within the interval  $[3, 3.2]$   $\text{W.m}^{-2}.\text{K}^{-1}$  (referred to as the "core" of  $\pi$ ) with no preference inside this interval. We find the conservative but not very informative values within  $[2.86, 3.33]$   $\text{W.m}^{-2}.\text{K}^{-1}$ , also known as the "support" of  $\pi$ . Intervals  $\pi_\theta$  containing values that have a level of possibility of at least  $\theta$  (lying between 0 and 1) are called  $\theta$ -cuts (see Figure 1). The wider the interval is, the more values judged to be unlikely are included, but the surer the true value belongs within this interval. Numerical possibility distribution may also be viewed as a nested set of confidence intervals, which are the  $\theta$ -cuts  $\pi_\theta = \{x, \pi(x) \geq \theta\}$  of  $\pi$ . The degree of certainty that  $\pi_\theta$  contains  $h$  is  $1 - \theta$ , *i.e.*,  $P(h \in \pi_\theta) \geq 1 - \theta$  or  $P(h \in \mathbb{R} \setminus \pi_\theta) \leq \theta$  (see Figure 1). Possibility distribution encodes a probability family (De Cooman and Aeyels, 1999; Dubois and Prade, 1992) limited by an upper probability bound known as the possibility measure  $\Pi(A) = \sup_{x \in A} \pi(x)$  (see the upper cumulative probability bound on Figure 1) and a lower probability bound known as the necessity measure  $N(A) = \inf_{x \notin A} (1 - \pi(x))$  (see the lower cumulative probability bound on Figure 1).

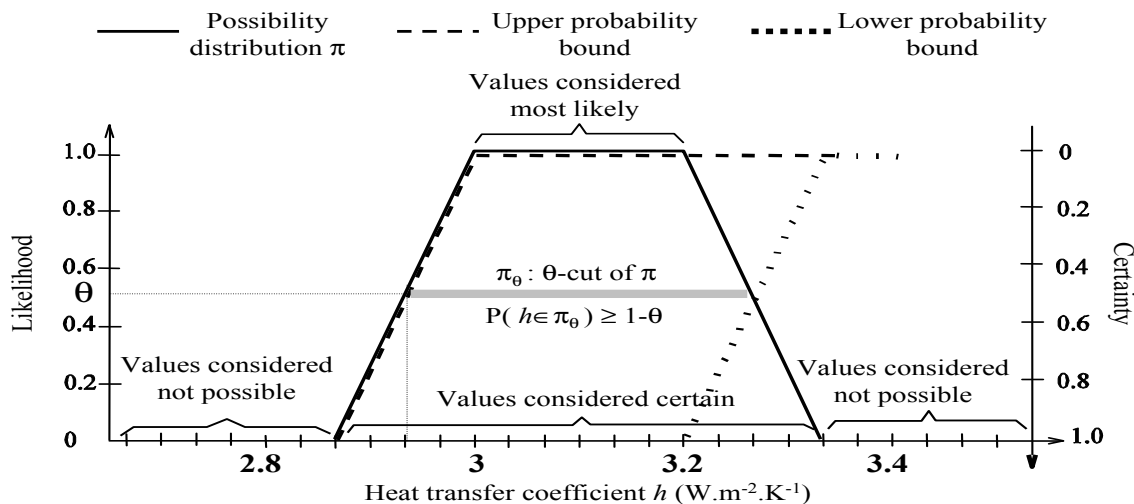


Figure 1. An example of a possibility distribution induced from the expert knowledge of heat transfer coefficient  $h$

### 3.2 Basic notion of belief functions induced from random sets

Belief functions (Dempster, 1967; Shafer, 1976) allow variability and imprecision to be treated within a single framework. While the probability theory assigns probability weights (in the discrete case) or probability density weights (in the continuous case) to each possible value of a parameter, the theory of belief functions may assign such weights to subsets of values (for example, intervals given by a sensor with a random and systematic error). A mass function  $\nu$  is thus defined, which assigns a weight  $\nu(A)$  to each subset  $A$  of values of the concerned parameter. Such a subset with positive weight is called a focal set. The weight  $\nu(A)$  is a probability mass that would be shared among specific values within  $A$  in the ideal case (rich information), but which remains unassigned due to imprecision in the case of poorer information. Belief functions provide two indicators to qualify the validity of a proposition stating that the value of the parameter lies within a prescribed set  $B$ . These indicators are the degree of belief of  $B$ ; referred to as  $Bel(B)$ , and the degree of plausibility; referred to as  $Pl(B)$  defined by Shafer (1976) as follows:

$$Bel(B) = \sum_{A, A \subseteq B} \nu(A) \quad \text{and} \quad Pl(B) = \sum_{A, A \cap B \neq \emptyset} \nu(A). \quad (1)$$

$Bel(B)$  gathers the imprecise evidence that asserts  $B$ ;  $Pl(B)$  gathers the imprecise evidence that does not contradict  $B$ . The interval  $[Bel(B), Pl(B)]$  contains all potential probability values induced by the mass function  $\nu$ . Within this scope,  $Bel(B)$  is the minimum amount of probability that must be assigned to  $B$  by sharing the probability weights defined by the mass function among single values in the focal sets.  $Pl(B)$  is the maximal amount of probability that can be likewise assigned to  $B$ .

Belief functions encompass possibility and probability theories in the discrete case. Hence, we can encode a probability distribution  $p$  and a possibility distribution  $\pi$  by using a mass distribution  $\nu$ . In the continuous case, the representation will be approximate in a discrete framework in order to do computations.

#### 1. Probability $\rightarrow$ Belief function.

Let  $X$  be a real random variable. In the discrete case, focal sets are singletons  $(\{x_i\})_i$  and the mass distribution  $\nu$  is defined by  $\nu(\{x_i\}) = P(X = x_i)$ . In the continuous case, focal intervals  $((x_i, x_{i+1}])_i$  are defined by discretizing probability density into  $m$  intervals and a mass distribution  $\nu$  is defined by  $\nu((x_i, x_{i+1}]) = P(X \in (x_i, x_{i+1}])$ ,  $\forall i = 1 \dots m$ .

#### 2. Possibility $\rightarrow$ Belief function.

Let  $X$  be a ill-known quantity described by a possibility distribution  $\pi$ . Focal sets correspond to the  $\theta$ -cuts

$$\pi_{\theta_j} = \{x | \pi(x) \geq \theta_j\}, \quad \forall j = 1 \dots q \quad (2)$$

of possibility distribution  $\pi$  associated with  $X$  so that  $0 < \theta_1 \geq \theta_j \geq \theta_{j+1} \geq \theta_q = 1$  and  $\pi_{\theta_{j+1}} \subseteq \pi_{\theta_j}$ . Mass distribution  $\nu$  is defined by  $\nu(\pi_{\theta_j}) = \theta_j - \theta_{j-1} \quad \forall j = 1 \dots q$  where  $\theta_0 = 0$ .

In the following, uncertainties were processed within the homogeneous framework of belief functions.

### 3.3 Practical propagation of uncertainty through a mathematical model

This section is devoted to briefly describing the combination and the propagation of three kinds of knowledge through a mathematical model: pure random variables, imprecisely known fixed

quantities and constant parameters (see Baudrit *et al.* (2007) for more details about the joint propagation methods of variability and imprecision). Consider a mathematical model  $m$  described by a function  $f$  depending on uncertain parameters  $(x_1, \dots, x_k, x_{k+1}, \dots, x_n)$ . To estimate the uncertainty on  $m$ , it is assumed that uncertainty related to  $(x_1, \dots, x_k)$  is quantified by single probability distributions  $(p^{x_1}, \dots, p^{x_k})$ , whereas uncertainty related to  $(x_{k+1}, \dots, x_n)$  is represented by possibility distributions  $(\pi^{x_{k+1}}, \dots, \pi^{x_n})$ . The propagation method is based on an extension of the well-known Monte-Carlo approach (Gentle, 1985) whereby sampling is performed both on random variables and on the  $\theta$ -cuts of the possibility distributions associated with each imprecise parameters. The outline of the method is summarized below:

1. A size  $L$  of the input sample is selected.
2. A random sampling is performed among focal sets (singleton for probability and interval for possibility, see Section 3.2) by taking known dependencies into account:

$$\begin{pmatrix} x_1^1 & \dots & x_k^1 & \pi_{\theta_{k+1,1}}^{x_{k+1}} & \dots & \pi_{\theta_{n,1}}^{x_n} \\ \vdots & \vdots & \vdots & \vdots & \vdots & \vdots \\ x_1^L & \dots & x_k^L & \pi_{\theta_{k+1,L}}^{x_{k+1}} & \dots & \pi_{\theta_{n,L}}^{x_n} \end{pmatrix} \quad (3)$$

where the interval  $\pi_{\theta_{j,i}}^{x_j}$  corresponds to the  $\theta_{j,i}$ -cut of the possibility distribution  $\pi^{x_j}$  with  $i = (1, \dots, L)$ , and  $j = (k+1, \dots, n)$ .

3. Propagating the sample through the model  $m$  requires the calculation of the lower and upper limits of  $m$ . Thus a random set with focal sets  $[\underline{m}_i, \overline{m}_i]_{i=1, \dots, L}$  is obtained and defined by:

$$\underline{m}_i = \inf_{(x_{k+1}, \dots, x_n) \in \pi_{\theta_{k+1,i}}^{x_{k+1}} \times \dots \times \pi_{\theta_{n,i}}^{x_n}} f(x_1^i, \dots, x_k^i, x_{k+1}, \dots, x_n) \quad (4)$$

and

$$\overline{m}_i = \sup_{(x_{k+1}, \dots, x_n) \in \pi_{\theta_{k+1,i}}^{x_{k+1}} \times \dots \times \pi_{\theta_{n,i}}^{x_n}} f(x_1^i, \dots, x_k^i, x_{k+1}, \dots, x_n) \quad (5)$$

4. According to Section 3.2, the empirical lower ( $Bel$ ) and upper ( $Pl$ ) probability bounds of the event  $\{m \in B\}$  from focal sets  $[\underline{m}_i, \overline{m}_i]_{i=1, \dots, L}$  are estimated by:

$$Bel(m \in B) = \frac{1}{L} \text{Card}\{i | [\underline{m}_i, \overline{m}_i] \subseteq B\} \quad (6)$$

and

$$Pl(m \in B) = \frac{1}{L} \text{Card}\{i | [\underline{m}_i, \overline{m}_i] \cap B \neq \emptyset\} \quad (7)$$

where  $B \subseteq \mathbb{R}$ .

The gap between  $Bel$  and  $Pl$  reflects the imprecise character of uncertainty related to the model  $m$ , thus creating an image of the extent of what is ignored.

## 4 Application description

### 4.1 Cheese making and ripening chambers

Camembert-type cheeses making was performed using the protocol described by Leclercq-Perlat *et al.* (2004). After drainage, the moulded cheeses were transferred into two ripening chambers, H1 and H2, of 0.91 and 0.63  $m^3$  respectively. Ripening time was about 14 days. Saint Nectaire type cheeses were manufactured at the INRA's Aurillac research centre, according to a technology similar to those of industrial Saint-Nectaire cheese production, as described in Picque *et al.* (2009). Two pilot ripening rooms,  $H_3$  and  $H_4$ , of 4.2  $m^3$  were used to perform the trials. Ripening time was of 28 days. A cheese washing performed on day 7 increased the cheese mass from 4 to 12 g depending on the trial.

### 4.2 Run description and data acquisition

A set of 10 trials - 8 for Camembert type cheese,  $C_1$  to  $C_8$ , and 2 for Saint Nectaire type cheese,  $SN_1$  to  $SN_2$  - was carried out. The cheeses were ripened inside rooms  $H_1$  to  $H_4$ , under controlled temperature and relative humidity conditions reported in Table 1, with accuracies of  $\pm 1^\circ C$  and  $\pm 2\%$  respectively. In the ripening rooms, the  $CO_2$  concentration was automatically maintained between 0.05 and 0.3% by air injection, Picque *et al.* (2006, 2009). The whole Camembert type cheese and Saint Nectaire type cheese runs were performed with continuous air ventilation.

Run	$C_1$	$C_2$	$C_3$	$C_4$	$C_5$	$C_6$	$C_7$	$C_8$	$SN_1$	$SN_2$
Ripening chamber	$H_1$	$H_2$	$H_1$	$H_2$	$H_1$	$H_2$	$H_1$	$H_2$	$H_3$	$H_4$
Temperature $^\circ C$	12	12	8	8	16	16	12	12	10	10
Relative humidity %	92	92	98	88	98	88	95	88	95	95

Table 1. Ripening chamber and control set points for Camembert ( $C_i$ ) and Saint Nectaire ( $SN_i$ ) trials.

The system used for the monitoring of the ripening rooms was composed of sensors and software as described in Picque *et al.* (2006, 2009). The sensors allowed the measurement of the chambers temperature, relative humidity,  $CO_2$  and  $O_2$  concentrations and of the cheese weight.

### 4.3 Model description

The model presented here was originally designed to study the cheese mass loss for a Camembert type cheese Hélias *et al.* (2007). A generalised model was developed, considering : (i) two different cheese technologies and sizes (Camembert-type soft cheese and Saint Nectaire-type pressed non-cooked cheese), (ii) a large range of trials (8 for each cheese type) involving significant changes in experimental ripening temperature and relative humidity, (iii) different conditions in ripening room size and air flow monitoring. The generalisation has been detailed in Gaucel *et al.* (2009) and in Deliverable D2A.3.8 (Mathematical model describing the dynamic of the Saint-Nectaire cheese type weight loss as a function of key environmental variables acting on the process. Proposition of ripening conditions improving the process). Only an overview of the model is described below. Model of mass loss was established from the combination of three phenomena: water evaporation, convective and radiant exchanges and respiratory activity. Biological activities are characterized by an oxygen consumption  $r_{O_2}$  and a carbon dioxide production  $r_{CO_2}$  ( $\text{mol}\cdot\text{m}^{-2}\cdot\text{s}^{-1}$ ), which induce gas exchanges between the cheeses and the ripening chamber atmosphere. The matter flux  $\phi_r$

( $\text{kg.m}^{-2}.\text{s}^{-1}$ ) linked to respiration is obtained by the difference between these two rates ( $r_{O_2}$ ,  $r_{CO_2}$  obtained from the derivatives of  $O_2$ ,  $CO_2$  concentration), balanced by the respective molar masses  $w_{O_2}$  and  $w_{CO_2}$  ( $\text{kg.mol}^{-1}$ )

$$\phi_r = w_{O_2}r_{O_2} - w_{CO_2}r_{CO_2}. \quad (8)$$

The difference between water vapour pressure in the atmosphere and at the cheese surface causes an evaporative flux  $\phi_w$ , traditionally represented as follows:

$$\phi_w = k (a_{ws}P_{sv}(T_s) - rhP_{sv}(T_\infty)) \quad (9)$$

where  $a_{ws}$  is the cheese surface water activity,  $T_s$  and  $T_\infty$  the average surface and atmospheric temperatures (K),  $rh$  the relative humidity (expressed between 0 and 1),  $P_{sv}(\cdot)$  (Pa) the saturation vapour pressure, and  $k$  the average water transfer coefficient ( $\text{W.Pa}^{-1}.\text{s}^{-1}$ ). The saturation vapour pressures  $P_{sv}(\cdot)$  are traditionally calculated with empirical relationships such as the Goff-Gratch equation (World Meteorological Organization, 2000).

Direct heat exchanges between the cheese and the atmosphere result from convective and radiative fluxes

$$\psi_{cr} = h (T_s - T_\infty) + \epsilon\sigma (T_s^4 - T_\infty^4) \quad (10)$$

where  $h$  is the average convective heat transfer coefficient ( $\text{W.m}^{-2}.\text{K}^{-1}$ ),  $\epsilon$  the product emissivity (dimensionless) and  $\sigma$  the Stefan-Boltzmann constant ( $\text{W.m}^{-2}.\text{K}^{-4}$ ). In addition, the moisture loss induces a heat consumption flux  $\psi_w = \lambda\phi_w$  for evaporation, with  $\lambda$  the latent heat of water evaporation ( $\text{J.kg}^{-1}$ ).

Cheese mass loss and cheese surface temperature can thus be represented by the following dynamic system (S) (Hélias *et al.*, 2007):

$$(S) : \begin{cases} \frac{dT_s}{dt} &= \frac{s}{mC}(-\psi_{cr} - \psi_w + \alpha \frac{r_{O_2} + r_{CO_2}}{2}) \\ \frac{dm}{dt} &= s(\phi_r - k\phi_w) \end{cases} \quad (11)$$

where  $m$  is the mass of a cheese (kg),  $s$  the surface exchange of the cheese ( $\text{m}^2$ ),  $C$  the specific heat ( $\text{J.kg}^{-1}.\text{K}^{-1}$ ) and  $\alpha$  the respiration heat ( $\text{J.mol}^{-1}$ ) induced by considerable mycelial development on the rind and determined according to the generic glucose respiration value (Kang and Lee, 1998).

## 5 Knowledge representation

In this section, an attempt to represent the available information relative to input variables and model parameters was done.

### 5.1 Model parameters

Knowledge about heat respiration  $\alpha$ , latent heat of water evaporation  $\lambda$ , product emissivity  $\epsilon$ , the Stefan-Boltzmann constant  $\sigma$  and the molar masses  $w_{CO_2}$  and  $w_{O_2}$  were taken from the literature (Kang and Lee, 1998; Mirade *et al.*, 2006; Perry, 1997). Surface water activity  $a_{ws}$  is a key parameter for equation (9). The specific heat  $C$  was determined experimentally. Common variables for Camembert and Saint Nectaire type cheeses are summarized in Table 2.

input	Source of information	Value
$C$ (J.kg <sup>-1</sup> .K <sup>-1</sup> )	Experimental determination	$2.194 \times 10^3$
$w_{CO_2}$ (kg.mol <sup>-1</sup> )	Literature	$4.4 \times 10^{-2}$
$w_{O_2}$ (kg.mol <sup>-1</sup> )	Literature	$3.2 \times 10^{-2}$
$\alpha$ (J.mol <sup>-1</sup> )	Literature (Kang and Lee, 1998)	$4.693 \times 10^{-5}$
$\lambda$ (J.kg <sup>-1</sup> )	Literature (Perry, 1997)	$2.47 \times 10^6$
$\epsilon$ (unitless)	Literature (Mirade <i>et al.</i> , 2004)	0.91
$\sigma$ (W.m <sup>-2</sup> .K <sup>-4</sup> )	Literature (Perry, 1997)	$5.67 \times 10^{-8}$

Table 2. Values and sources for common parameters for both Camembert and Saint Nectaire type cheeses.

The surface area of cheese  $s$  was also determined experimentally with range of values given in Table 3, which are assumed to be reliable.

Based on the lack of knowledge and measurements relative to cheese surface water activity,  $a_w$ , this parameter was represented by intervals [0.964, 0.984] (from (Hélias *et al.*, 2007)) and [0.96, 0.99] (unpublished data) for Camembert and Saint Nectaire type cheese, respectively. Due to low airflow velocity (lower than 0.1 m.s<sup>-1</sup> for Camembert trials and in the range  $0.16 \pm 0.06$  m.s<sup>-1</sup> for Saint Nectaire trials) inside ripening chambers, the heat transfer coefficient  $h$  cannot be determined by the relationship presented in Mirade *et al.* (2004). Experts consider that the heat transfer coefficient for ripening rooms  $H_1$  and  $H_2$  (Camembert trials) is most likely in [1.1, 1.5] and [1.6, 2.4] (W.m<sup>-2</sup>.K<sup>-1</sup>) for rooms  $H_1$  and  $H_2$  respectively. However, they do not exclude values as low as 1 - case of non-stirred chamber (Kondjoyan, 2009) - and as high as 4 W.m<sup>-2</sup>.K<sup>-1</sup>. For Saint Nectaire type cheese, experts conclusions leads to most likely values in [5.2, 7] without excluding values in the larger range [4, 8].

The knowledge of convective heat transfer coefficient  $h$  is then represented by means of a possibility distribution of cores [1.1, 1.5], [1.6, 2.4] and support [1, 4], for Camembert trials, and cores [5.2, 7], support [4, 8] for Saint Nectaire trials as depicted in Figure 2.

The following relationship between  $h$  and  $k$  was established by Mirade *et al.* (2004):

$$k = 0.66.10^{-8}h^{1.09} \quad (12)$$

According to equation (12) and using fuzzy interval analysis (Dubois *et al.*, 2000), knowledge about the average water transfer coefficient  $k$  is also represented by a possibility distribution. Fuzzy interval analysis can be thought of simply as classical interval calculus performed at different levels of possibility.

## 5.2 Input variables

The dynamical system  $S$  (equation 11) depends on four input variables that describe the gas exchanges ( $r_{O_2}, r_{CO_2}$ ) between the cheese and the atmosphere, and the climatic conditions ( $T_\infty, rh$ ). It was assumed that sensors measuring temperature  $T_\infty$  and gas exchanges ( $r_{O_2}, r_{CO_2}$ ) were reliable and give relatively precise measures. However, it is very difficult to measure relative humidity  $rh$  inside chambers. Consequently, a maximal measurement error of  $\pm 1\%$  was considered, and the error on  $rh$  measurement was supposed to follow a Beta law  $Beta(5, 5)$ .

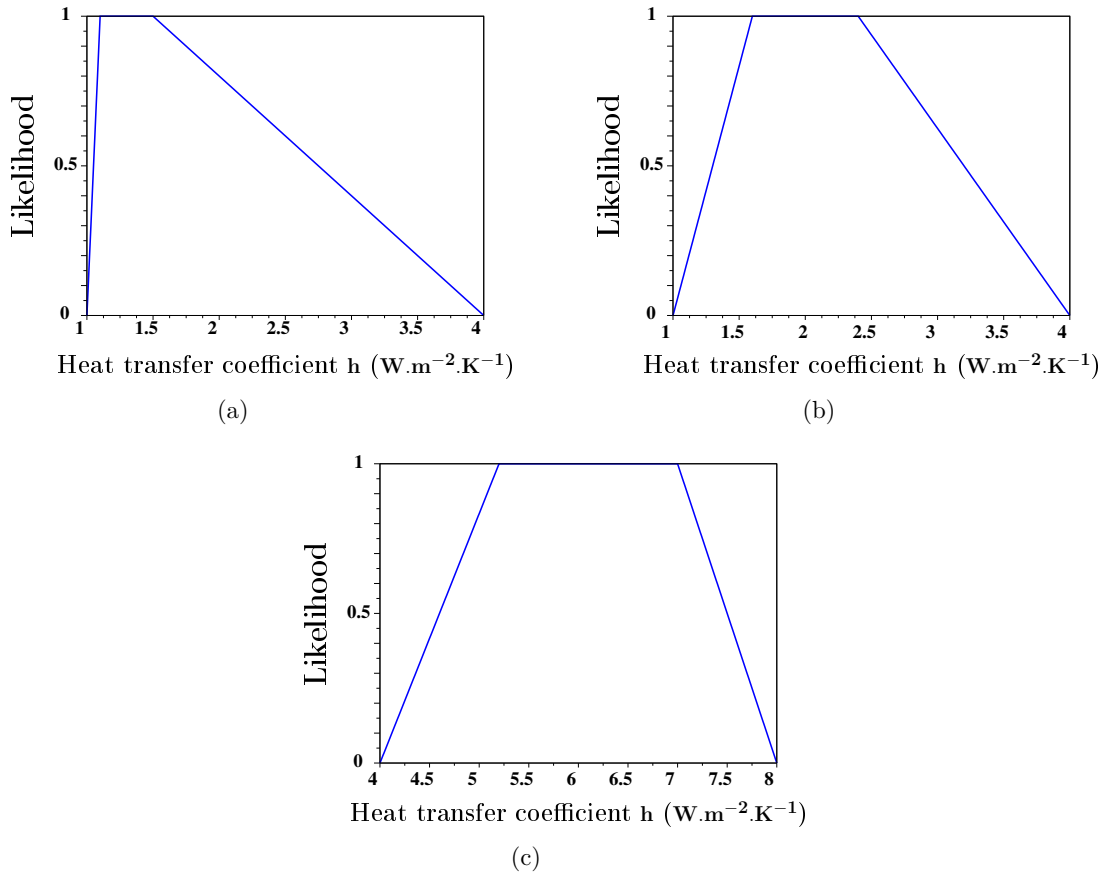


Figure 2. Possibility distribution representing knowledge about the heat transfer coefficient  $h$  for Camembert (ripening chamber  $H_1$  (a) and ripening chamber  $H_2$  (b) ) and Saint Nectaire (c)

Table 3 summarizes the representations of input variables and parameters of the cheese mass loss model for Camembert and Saint Nectaire type cheese.

Input	Source of information	Mode of representation	
		Camembert	Saint-Nectaire
$a_{ws}$ (unitless)	Experimental determination	interval [0.964, 0.984]	interval [0.96, 0.99]
$h$ ( $\text{W}\cdot\text{m}^{-2}\cdot\text{K}^{-1}$ )	Sparse measurements and expert opinion	Possibility distribution	
		room $H_1$ : support=[1, 4] core=[1.1, 1.5]	support=[4, 8] core=[5.2, 7]
		room $H_2$ : support=[1, 4] core=[1.6, 2.4]	
$k$ ( $\text{kg}\cdot\text{m}^{-2}\cdot\text{Pa}^{-1}\cdot\text{s}^{-1}$ )	Relationship with $h$	Possibility distribution	
$s$ ( $10^{-2} \text{ m}^2$ )	Experimental determination	range [2.79, 2.88]	range [9.43, 9.46]
$T_\infty$ (K)	Reliable Measurements	online data	
$rh$ (unitless)	Measurements	error distribution $Beta(5, 5)$	

Table 3. Summary of knowledge about specific parameters, control variables and selected modes of representation for Camembert and Saint Nectaire.

### 5.3 Known and assumed dependencies

Explicit dependencies exist between parameters and input variables, as following:

- At a fixed  $h$ ,  $k = 0.66 \cdot 10^{-8} h^{1.09}$ .
- Relative humidity  $rh$  and temperature  $T_\infty$  are considered independent.
- The group of input variables ( $rh, T_\infty$ ) and the group of parameters ( $h, k$ ) are considered independent.

## 6 Results

In this section, the imprecise nature of available information regarding the heat and water transfer coefficient and cheese surface water activity was taken into account. An attempt to jointly propagate variability and imprecision in the estimation of cheese mass loss through the ripening process for 8 trials for Camembert and 2 trials for Saint Nectaire was carried out (see methodology in Sections 3.2 and 3.3). For this application, according to the non-monotony of the model, the Simulated Annealing Meta-Heuristic was used to estimate the maximal and minimal final cheese mass obtained by equations 4 and 5. As described in section 3.3, a set of upper and lower final mass was calculated. Thus, estimated upper (Pl) and lower (Bel) probabilities were derived by using equations 6 and 7. See Figure 3 for the lower (*Bel*) and upper (*Pl*) cumulative probability bounds of the cheese mass loss at day 14 for trial  $C_2$ . This figure allows to visualize to what extent the final mass is at least / at worst lower than a certain treshold.

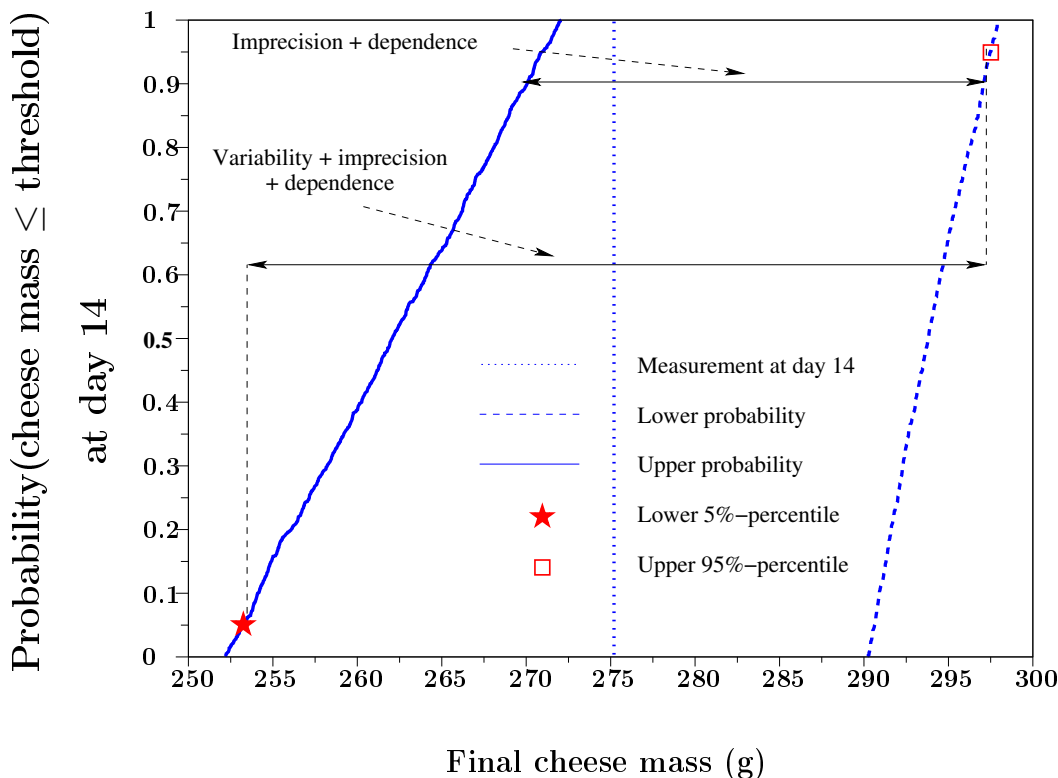


Figure 3. Lower and Upper probabilities that cheese mass is lower than a certain weight at day 14 for trial  $C_2$  with an initial mass of 315.9 g.

The gap between these two limits is primarily a consequence of the imprecise nature of available information about the transfer coefficients  $h$  and  $k$  and the cheese surface water activity  $a_w$  and, to a lesser extent, of the choice of the dependence in the propagation method.

According to Figure 3, there is a 5% plausibility of being lower than 253.3 g, and a 95% belief of being lower than 297.5 g. That means that we are 95% sure that the final mass of cheeses does not exceed 297.5g. On the other hand, we are 95% sure that the cheeses final mass is at least of 253.3 g before being packaged.

The confidence bounds on the cheese mass loss at the end of the ripening are summarized in Tables 4 and 5 for Camembert and Saint Nectaire respectively, and compared to experimental mass loss. For Camembert type cheese (Table 4), the length of the cheese mass loss ranges vary from 14.2 g - for low water exchange and biological activity induced by high value of relative humidity (98%) and low temperature (8°C) - to 71.6 g - for high water exchange and biological activity induced by low value of relative humidity (88%) and high temperature (16°C). Results for the Saint Nectaire experiments leads to similar length of the mass loss ranges, about 300g, for trials  $E_1$  and  $E_2$ . Corresponding figures for the lower ( $Bel$ ) and upper ( $Pl$ ) cumulative probability curves are given in the appendix (Figures 4, 5 and 6). These figures show a strong dependence between the slope of the ( $Bel$ ) and ( $Pl$ ) cumulative probability curves and the shape of the possibility distribution representing the expert's knowledge for the heat transfer  $h$ . As an example, for the ripening chamber  $H_1$  (Figure 4), the lower bounds of the support and the core are quite similar (1 and 1.1 respectively), thus the slope of the lower ( $Bel$ ) probability curve is close to 1.

Trial	Ripening conditions		Experimental results		Confidence values (95%)	
	Room	( $T, rh$ )	Initial cheese mass (g)	cheese mass loss (g)	maximal cheese mass loss (g)	minimal cheese mass loss (g)
$C_1$	$H_1$	12°C, 92%	310.2	32.6	71.8	23.9
$C_2$	$H_2$	12°C, 92%	315.9	40.7	62.6	18.4
$C_3$	$H_1$	8°C, 98%	297.5	15.0	21.4	7.2
$C_4$	$H_2$	8°C, 88%	302.8	42.5	70.6	20.4
$C_5$	$H_1$	16°C, 98%	314.5	33.6	48.2	19.5
$C_6$	$H_2$	16°C, 88%	320.3	60.5	106.4	34.8
$C_7$	$H_1$	12°C, 95%	320.2	23.1	36.9	11.6
$C_8$	$H_2$	12°C, 88%	320.1	45.4	86.8	27.6

Table 4. Confidence values at 95% of minimal and maximal cheese mass loss according to the environmental conditions of the Camembert-type cheese ripening and comparison with the experimental values

As a first conclusion, these results show that taking into account uncertainties do not mask effect of the ripening control variables ( $T, rh$ ) onto the cheese mass dynamic.

Nevertheless, in both Camembert and Saint Nectaire results, the maximal cheese mass loss can be considered as too high by industrial cheesemakers to be used as a production control tool. A solution to overcome this effect can be to refine the available knowledge on the heat transfer coefficient  $h$  and/or on the cheese surface water activity  $a_w$ .

Trial	Ripening conditions		Experimental results		Confidence values (95%)	
	Room	$(T, rh)$	Initial cheese mass (g)	cheese mass loss (g)	maximal cheese mass loss (g)	minimal cheese mass loss (g)
$SN_1$	$H_3$	10°C, 95%	1709.7	208.4	343.4	53.4
$SN_2$	$H_4$	10°C, 95%	1697.8	197.1	372.8	68.1

Table 5. Confidence values at 95% of minimal and maximal cheese mass loss according to the environmental conditions of the Saint Nectaire -type cheese ripening and comparison with the experimental values

## 7 Conclusion

During cheese ripening, a mass loss occurs resulting from heat and mass transfers from the cheese to the atmosphere. This phenomenon is based on physical processes and biological activity. The state of knowledge about model food processes induces uncertainty about some phenomena and, as a consequence, about some model input variables and parameters. This work presents an application of an alternative uncertainty propagation method to calculate cheese mass loss during ripening where imprecise information is represented using possibility distributions (nested intervals). Such nested intervals are suited to the representation of expert knowledge because the expert can then be expected to be consistent with himself: the interval of values that he considers most likely is necessarily included within the interval outside of which he considers that values are not possible.

By assuming that the shape and the initial weights of all cheeses are quite similar, the treatment of uncertainties allows to estimate the global lower and upper bounds of final mass (or mass loss) for the whole production. As accurate mapping of ripening room airflow pattern is difficult and expensive to establish and simulate, a pilot scale ripening chamber with transfer coefficients in the same range than for industrial ripening appears as an interesting experimental approach. On the basis of a model calibrated for such a pilot scale, this approach could provide key information for improving the control of the mass loss of cheeses under industrial conditions.

Moreover, taking partial ignorance into account on the mathematical model that was established from a pilot scale can help us to transpose it onto an industrial scale. Propagating imprecision on the basis of shown results can help to improve the process control. It is interesting to observe that a strategy to complete this knowledge can be developed so as to be able to give a better estimation of the mass loss at the end of the ripening process. For example, considering the wide gap between the upper and lower bounds on probability in figures showned in the appendix, it is clear that further studies on transfer coefficients, cheese surface water activity and ripening chamber climatic conditions are necessary in order to reduce the subjective uncertainty regarding these factors.

## References

- Baudrit, C., Dubois, D. (2006). Practical Representation of Incomplete Probabilistic Knowledge. *Comput. Stat. Data Anal.*, 51(1), 86-108.
- Baudrit, C., Couso, I., Dubois, D. (2007). Joint Propagation of Probability and Possibility in Risk Analysis: toward a formal framework. *Int. J. of Appro. Reason.*, 45(1), 82-105.

- Baudrit C., Guyonnet, D., Dubois, D. (2007). Joint propagation of variability and imprecision in assessing the risk of groundwater contamination. *Journal of Contaminant Hydrology*, Volume 93, Issues 1-4, Pages 72-84.
- De Cooman, G., Aeyels, D. Supremum-preserving upper probabilities. (1999). *Information Sciences*, 118, 173-212.
- Dempster, A.P. Upper and Lower Probabilities Induced by a Multivalued Mapping. (1967). *Ann. Math. Stat.*, 38, 325-339.
- Dubois, D., Nguyen, H.T., Prade, H. (2000). Possibility theory, probability and fuzzy sets: misunderstandings, bridges and gaps. *Fundamentals of Fuzzy Sets*, Dubois,D. Prade,H., Eds: Kluwer , Boston, Mass, 343-438.
- Dubois, D., Prade, H. (1992). When upper probabilities are possibility measures. *Fuzzy Sets Syst.*, 49, 65-74.
- Ferson, S., Ginzburg, L.R. (1996). Different methods are needed to propagate ignorance and variability. *Reliability Engineering and Systems Safety*, 54, 133-144.
- Gaucel, S., Guillemin, H., Corrieu, G. (2009). A generalised model describing cheese mass loss during ripening. XIIème Congrès de la Société Française de Génie des Procédés (SFGP), Marseille.
- Gentle, J.E. (1985). Monte-Carlo methods. In S. Kotz and N.L. Johnson eds, editors, *Encyclopedia of Statistics*, 5, 612-617. John Wiley and Sons, New York.
- A. Hélias, P.-S. Mirade, and G. Corrieu. (2007). Modeling of Camembert-Type Cheese Mass Loss in a Ripening Chamber: Main Biological and Physical Phenomena *J. Dairy Sci.*,90, 5324-5333.
- Kang, J. S., and D. S. Lee. (1998). A kinetic model for transpiration of fresh produce in a controlled atmosphere. *J. Food Eng*, 35, 65-73.
- Kondjoyan, A. (2006). A review on surface heat and mass transfer coefficients during air chilling and storage of food products. *Int. J. Ref.* 29, 863-875.
- Leclercq-Perlat, M.N., and F. Buono and D. Lambert and E. Latrille and H.-E. Spinnler and G. Corrieu. (2004). Controlled production of Camembert-type cheeses. Part 1: Microbiological and physicochemical evolutions. *J. Dairy Res.*, 35, 346-354.
- Mirade P.-S., Rougier T., Daudin J.-D., Picque D. and Corrieu G. (2006). Effect of design of blowing duct on ventilation homogeneity around cheeses in a ripening chamber. *Journal of Food Engineering*, 75(1), 59-70.
- Mirade, P.S. and T. Rougier and A. Kondjoyan and J.D. Daudin and D. Picque & G. Corrieu. (2004). Caractérisation expérimentale de l'aéraulique d'un hâloir de fromagerie et des échanges air-produit. *Lait*, 84, 483-500.
- Perry, R.H., D.W. Green. (1997). *Perry's Chemical Engineers' Handbook*, McGraw-Hill. NY.
- Picque, D., and M.-N. Leclercq-Perlat and G. Corrieu. (2006). Effects of Atmospheric Composition on Respiratory Behavior, Weight Loss, and Appearance of Camembert-Type Cheeses During Chamber Ripening. *J.Dairy Sci.*, 89, 3250-3259.

- Picque, D., Guillemin, H., Mirade, P.-S., Didienne, R., Lavigne, R., Perret, B., Montel, M.-C., Corrieu, G. (2009). Effect of sequential ventilation on cheese ripening and energy consumption in pilot ripening rooms. *Int. Dairy J.* 19:489-497
- Shafer, G. (1976). *A Mathematical Theory of Evidence*. Princeton University Press.
- Smets P. and Kennes R. (1994). The transferable belief model. *Artificial Intelligence*, 66, 191-234.
- Walley, P. 1991. *Statistical Reasoning with Imprecise Probabilities*, Chapman and Hall, 1991.
- World Meteorological Organization. General meteorological standards and recommended practices, Appendix A, corrigendum. (2000). *World Meteorological Organization Technical Regulations*, Geneva, 49.

# Appendix A

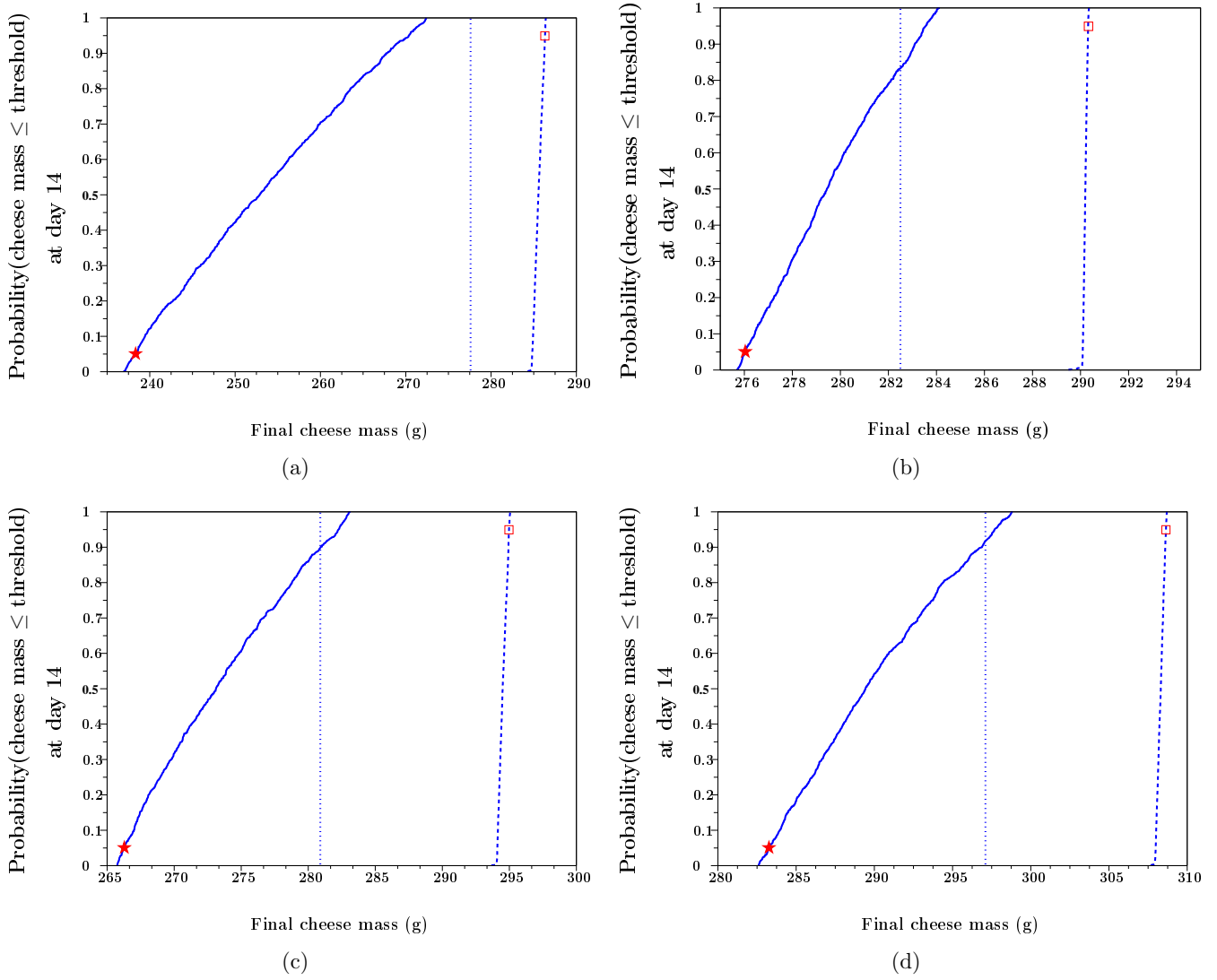


Figure 4. Results for Camembert (ripening chamber  $H_1$ ): trials  $C_1$  (a),  $C_3$  (b),  $C_5$  (c) and  $C_7$  (d). Thick line and dashed line correspond to upper and lower probabilities, respectively. Square ( $\square$ ) and star ( $\star$ ) symbols represent upper-95% and lower-5% percentiles. The vertical dotted line represents the measured final cheese mass after 14 days of ripening.

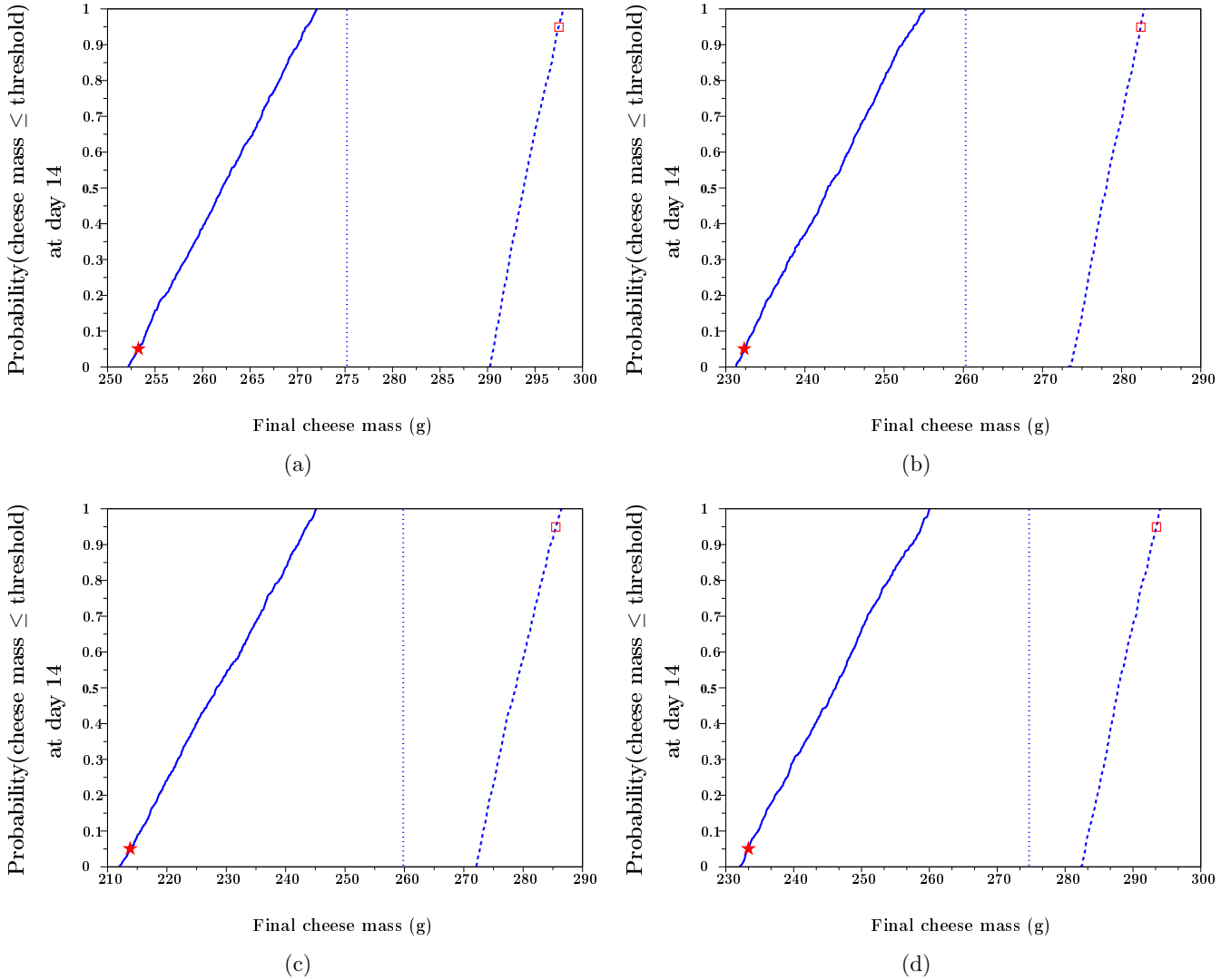


Figure 5. Results for Camembert (ripening chamber  $H_2$ ): trials  $C_2$  (a),  $C_4$  (b),  $C_6$  (c) and  $C_8$  (d). Thick line and dashed line correspond to upper and lower probabilities, respectively. Square ( $\square$ ) and star ( $\star$ ) represent upper-95% and lower-5% percentiles. The vertical dotted line represents the measured final cheese mass after 14 days of ripening.

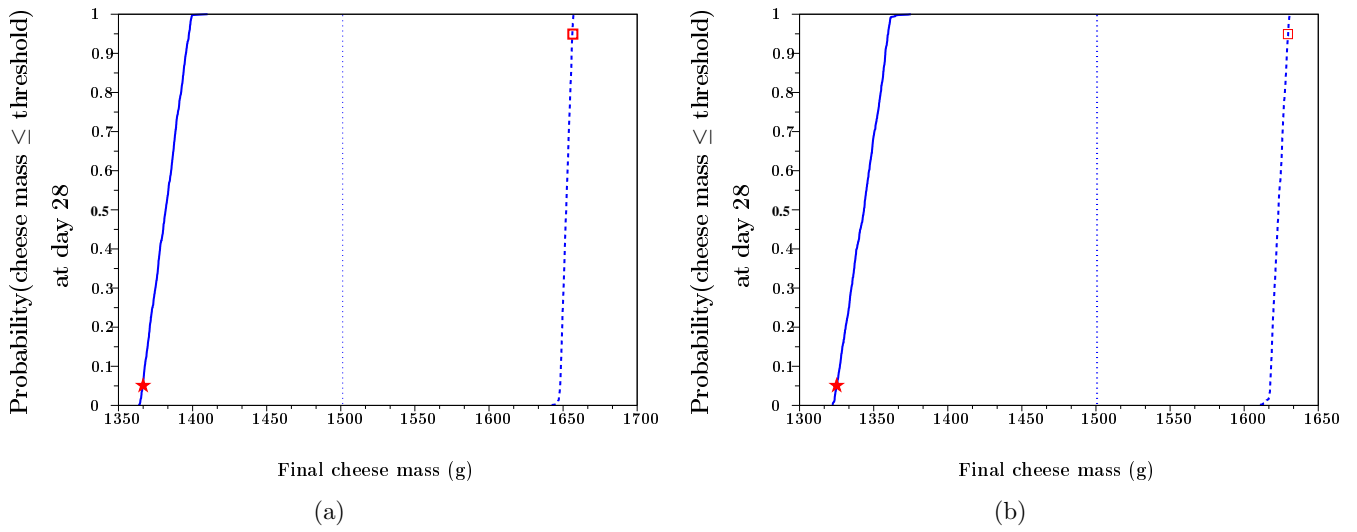


Figure 6. Results for Saint Nectaire: trials  $SN_1$  (a) and  $SN_2$  (b). Thick line and dashed line correspond to upper and lower probabilities, respectively. Square ( $\square$ ) and star ( $\star$ ) represent upper-95% and lower-5% percentiles. The vertical dotted line represents the measured final cheese mass after 28 days of ripening.